Engineering Journal issn: 0125-8281

Article

Advanced Production Separator for Crude Oil Production in Thailand

Kawin Sonthipermpoon[1,*], Kwanchai Kaitong[2], Wikorn Punyain[3], Yupin Phuphuak[3], and Somchai Kongnoo[1]

1 Department of Industrial Engineering, Faculty of Engineering, Naresuan University, Phitsanulok, Thailand
2 Department of Mechanical Engineering, Faculty of Engineering, Naresuan University, Phitsanulok, Thailand
3 Department of Chemistry, Faculty of Science, Naresuan University, Phitsanulok, Thailand
*E-mail: sonkawin@nu.ac.th (Corresponding author)

Abstract. The propose is a new design and development of an advanced separator for oil production in Thailand on a prototype scale to order avoid deposition of sand contaminated include oil production. The novel separator was designed by installing a series of impellers along the horizontal bottom of the separator. The system was successfully implemented on the laboratory scale. A computational fluid dynamics (CFDs) model is employed to investigate the 3D hydrodynamics and flow behavior inside the separator tank modified with impellers. The CFD simulation was operated for 300 min. It could fundamentally demonstrate the flow phenomena of the crude fluids that the sand flowing out from the separator through the water outlet part depends on the accumulation of sand packing bed near the open channel of the outlet and including the effect of impeller rotation. It also shows the wave pattern of the sand outlet and the movement of the impeller did not disturb the efficiency of oil-water phase separation. In the laboratory experiments, the optimum conditions for sand separation in the water outlet part were investigated in terms of impeller sizes, the rotational speed of impellers, and the effect of duration times. The impeller sizes were compared between 3 inches and 5 inches in diameter. The results show that 5 inch-impeller is the optimum size for preventing the sand packing in this system. It was found that 200 rpm gave the most powerful speed of rotation to remove sand to the open channel. From all over the results of the CFD simulation and lab experiment, it could be concluded that the separator system with a strong rotation of impellers leads to effectively prevent sand sedimentation in the separator.

Keywords: Production separator, filter sand, hydro cyclone, computational fluid dynamics, design of experiments.

ENGINEERING JOURNAL Volume 26 Issue 12
Received 22 December 2021
Accepted 19 December 2022
Published 29 December 2022
Online at https://engj.org/
DOI:10.4186/ej.2022.26.12.1

DOI:10.4186/ej.2022.26.12.1

1. Introduction

In the oil production business, crude oil is usually composed of oil, gas, water, and impurities (depending on the reservoir location) such as sediment or sand, and sometimes hydrogen sulfide. Before the oil can be sold or delivered into a tank storage or pipeline, these impurities, especially sand, must be removed to bring the crude up to the proper quality. Generally, a Production separator is used as equipment to separate water and oil in petroleum production. For a long time of this process, sand tends to have very dense packing and thicker deposition in the bottom of the separator which is very difficult to be removed. Sand deposition becomes a chronic problem in the oil and gas business in terms of erosion, low separation performance, additional downtime for sand cleaning, reducing equipment integrity, additional maintenance cost, and waste management cost. These facts have attracted the attention of academic and industrial areas, enabling the appearance of new technologies or improvement of the water/oil/sand separation process.

"PTTEP filed Thai and US patent" aims to solve sand deposition under the core concept and uniqueness: "Impeller are installed to prevent sand sedimentation by creating turbulence while maintaining oil-water separation with concerning areas that affect oil-water gas separation." A collaborative task force between PTTEP and Naresuan University has been formed to materialize this novel idea by developing a lab-scale prototype for the advanced separator.

This project focuses on the design and development of novel sand-oil separator to prevent sand accumulations in the separator which will be easy to be cleaned. Furthermore, this optimized system can be applied in pilot scale for oil production industries.

2. Literature Reviews

Sand deposit is one of the most serious problems in oil production not only for crude oil production in Thailand but also for every oil company all over the world. As we know, it is an impurity in crude oil from natural resources and is typically difficult to be isolated from the whole crude. It reduced the efficiency of outcome crude oil for further production and always makes machines and equipment decline by its accumulation. According to the above problem, there are many companies and scientists trying to find a solution for better production efficiency. Researches are diverse and can be divided into two types, the first is adding more steps to oil production, and the second is adding or developing the equipment to oil production. We did research and find that there're many developers who have been researching about this.

In 2002, Fort et al. [1]. studied modifying the configuration of vessels in petroleum production. This idea was not only to prevent the deposition of sand and other solids but maybe also to improve the flow rate and flow behavior as well. They suggested that applying a pitched blade impeller inside the vessel might help the fluid flow. Moreover, solids will not go down to the bottom of the vessel and start to pack. They also studied the appropriate configuration of the blade impeller and the position to install a blade in a vessel. The mean velocity was measured using laser Doppler anemometry in a transparent vessel of diameter T = 400 mm, provided with a standard dished bottom. Three and six-blade pitched blade impellers (the pitch angle varied within the interval α € <24°; 45°>) of impeller/vessel diameter ratio D/T = 0.36, as well as a three-blade pitched blade impeller with folded blades of the same diameter, were tested. The result showed that the most appropriate blade position has to be at the bottom of the vessel to prevent the deposition of sand. The factor that should be realized is the gap between the bottom of the vessel and the body of the blades. To solve this problem, they inserted the dish into that gap. The size and diameter of the blade depend on the environment of the vessel but they can identify one thing 'Three-blade is more effective' as shown in Fig. 1.

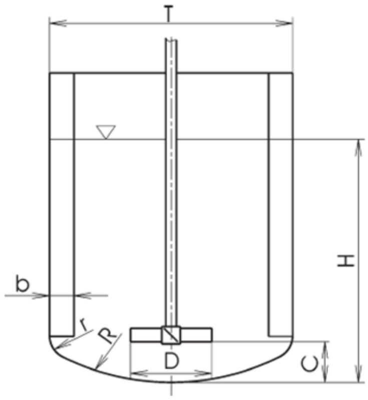

Fig. 1. Layout of test rig with dished bottom (H/T = 0.36, C/D = 0.5, b/T = 0.1, R/T = 0.1). [1].

Simmons et al. [2]. studied residence time distribution and flow behavior within primary crude oil-water separators. They believed that the residence time is significant to focus on but it might not have a constant time because of the various parameters from crude oil. There are many factors that can't be controlled by an operation such as viscosity, level of water-oil, and behavior of fluid that flow in separator which is in vessel shape.

Based on this fact, they studied that if they can control the behavior of fluid that agrees to appropriate residence time, it will be easier to adapt to other oil fields. Along with hydrodynamic rules they tried to add baffling in the vessel of the separator to control the behavior of the fluid. They set the baffling at the inlet pump and the bottom of the vessel to study the effects of baffling called alternative path model (APM). The model showed that vessel performance was affected by the internal configuration (flow smoothing baffles and separation plates) and the primary separation duty (gas-liquid or oil-water). The addition of baffle led to less turbulence of the flow for oil-water separation, but less so for gas–oil separation.

In 2005, Bibobra et al. [3]. also realized the problem of sand deposition. In the petroleum industry, there's no way to avoid sand and other contaminants that can come up from the natural wells in the oil field. Not even sand will deposition inside separator it will cause the erosion to industry facility as well.

This study was acquired in the Garon field which is in the Niger Delta to study about behavior and other physical properties of sand deposition. The result and data were collected and obtained with Clampon DSC to identify the effects of sand invasion on subsurface and surface production facilities. Also presented are the effects of sand invasion on the surface facility, choke, screen and tubing. Approximately 800 liters of sand were drained and recovered from the test separator. Comparing this quantity with the previously recovered sand at 64/64" on 1" trim choke (350 liters), the current sand quantity is higher than the former by 650 liters. The erosion of choke (surface), tubing, screen, cuts production of the flow line, loads of treating facilities, loss of production during work-over jobs, and loss of valuable man-hour during the period of close-in in terms of wages. Thousands of dollars were spent to carry out work over the operation as well as installation of the sand control measures. The result of the effect of sand production is shown in Fig. 2.

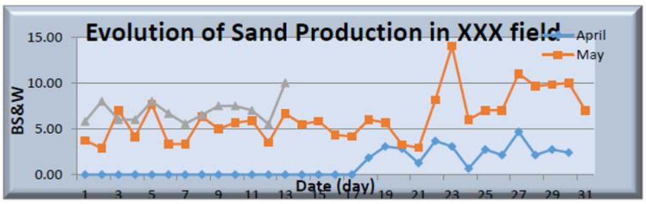

Fig. 2. Sand production evolution [3].

In 2006, Guo et al. [4]. studied the mechanism of sand removal from crude oil. They had a prediction that the sediment of sand might be up to many factors such as the various diameter of sand particles, different oil-water ratios, and viscosity of the oil. They wanted to do the paralleled experimental between the simulation and real experimental by using CFD software FLUENT. Field experiment held in China National Offshore Oil Corporation joining with Institute of Mechanics, CAS. Their result can be concluded that: (i) in case of highly viscous oil, the sedimentation of small sand particles was more difficult, (ii) centrifugal separation was more effective in the separation of small diameter sand particles, and (iii) for various oil viscosities, the separation efficiency of sand particles with diameters more than 100 eyes can reach 95 percent.

Goharzadeh et al. [5]. studied sand transportation by doing an experimental study of three-phase flows (air-water-sand) inside a horizontal pipe. The results obtained aim to enhance the fundamental understanding of sand transportation due to saltation in the presence of a gas-liquid two-phase intermittent flow. Sand dune pitch, length, height, and front velocity were measured using high- speed video photography. The result shows that Sand transportation was assessed for four flow compositions with differing gas ratios, including hydraulic conveying, having the same mixture velocity. However, for elongated bubble flow, the sand bed was transported further downstream relative to hydraulic conveying. It was also observed that the slug body significantly influences sand particle mobility.

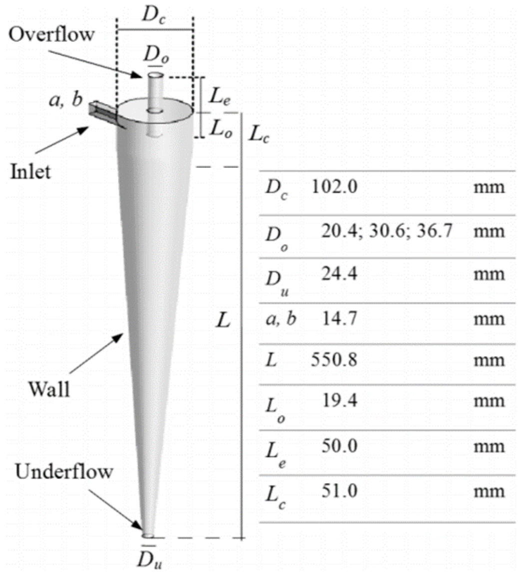

Fig. 3. Dimension of hydro cyclone [6].

Farias et al. [6]. investigated the effects of hydro cyclone in the separation of water-sand-oil in oil production to improve the efficiency of separation. They aimed and predicted that if they can generate a cyclone shape of water in a separator it will prevent the sediment of sand in the tank. They used the ANSYS software to simulate the operation and behavior in the separator. They found that the hydro cyclone can reduce the sediment of sand in the separator. However, the efficiency of the hydro cyclone was dependent on the diameter of the cyclone and the environment of crude oil such as particle size of sand, the difference between water-oil level, and volume of inlet sand mixed in crude oil.

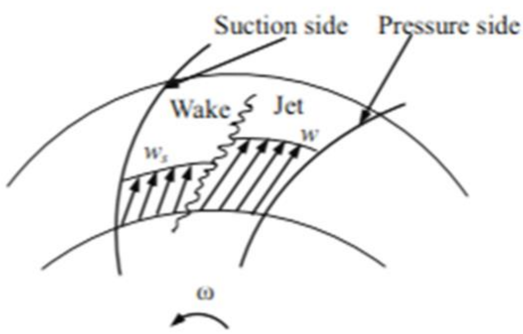

Fig. 4. Jet-wake flow pattern in impeller [7].

In 2016, Bellary et al. [7]. studied optimizing centrifugal impellers which use in the oil and gas industry. Centrifugal pumps are used in the oil and gas industry for a long time and the efficiency of pumping drops with higher viscosity and higher surface roughness. The hypothesis is a pump impeller and an impeller design have a significant effect on the pump performance. In this study, a 3D flow simulation was used with the Reynolds-averaged Navier–Stokes (RANS) equation to predict and analyze the behavior of crude oil pumping. They considered different blade angles and impeller surface roughness to pump crude oil, kerosene, gasoline, saline water, and water. The results showed that in the same angle and size of the impeller, the higher viscosity and higher surface roughness of liquid made it more difficult for pumping. The flow rate of the inlet might help but it also needed more power in the system to pump liquid.

Sanni et al. [8]. studied sand entrainment and deposits in horizontal oil transport. They realized that the drop in pressure within the lines, gives rise to sand traps. This paper examines a non-conventional method of sand management for the transport process which does not involve sand removal from the crude oil being transported. They focused on sand deposition problems use of a non-sand exclusion method to be controlling sand deposition in petroleum pipes against the conventional method. The new model was developed which aims at describing the laminar and turbulent flow behavior of sand and crude oil in the horizontal pipe between the head of a well and its flow station.

The equation is used to evaluate the molecular diffusivity of the mixture.

$$D = \frac{1}{6} \times d \times u' \quad (1)$$

where d = diameter of particle, D = molecular diffusivity (coefficient of diffusion), u' = average velocity of mix $((\varphi\omega_s+\varepsilon\omega_f)/2)$ that ω_s and ω_f = sand and fluid velocities, using the data given in Sanni et al, d = 0.05m, ω_s = 27.04 m/s and ω_f = 30.04 m/s: D = De = 0.2378 m^2/s (effective diffusivity)

Then, the effective diffusivity εT, is given as: $\varepsilon T = \varepsilon 1 + \varepsilon 2 + \varepsilon 3 = 0.000001395 + 0.000267893 + 0.002450926 = 0.00272\ m^2/s$

In 2017, Zhang et al. [9]. studied water and sand separation from crude oil by computer simulation. They use the Lao Junmiao oil field for the real data to compare with data analyzed from software. They focus on the importance of the environment in the settling tank such as settling time, temperature, and processing capacity. The experiment was held at 20°C and solved by FLUENT. The maximum relative error of the model simulation is 9.38% while the corresponding results of the Euler-Eulerian method solved are 33.46%. The results proved that processing capacity, settling time and temperature are significant for enhancing separation efficiency.

3. Research Methodology

On the basis of the above considerations, there are several ways to prevent sedimentation of sand. One of the most effective ways is development of the equipment by adding some internal part that seems to be the most promising choice to reduce this problem. However, up to the present, there is no report about installing impellers at bottom of separator to prevent sand deposit.

This research work originally proposes the innovative design of separator that contains internal impellers along the horizontal bottom of the separator with controlling speed of impeller rotation. The impeller was designed to have three blades according to report of Fort (Fort et al. 2002) by varying size and speed of rotation. Impeller with various sizes in diameter of 3, 4 and 5 inches will be compared to study the different efficiency. The speed of impeller rotation will be varied as: 0, 10, 50, 100 and 200 rpm. Duration time of running is extended to 300 minutes to see evolution of sand removal. CFD model is also performed to observe the moving pattern and hydrodynamic flow of fluids inside the prototype separator.

The goal of this research is to develop a new separator which is the first state for crude oil from natural well. If we could manage sand since up-stream it may be more comfortable to manage it in down-stream. This research metrology has about 2 processes are experimental setup and experimental method.

3.1. Experimental Setup

Instruction of laboratory scaled separator. The lab-scale separator for the experimental study was located in room 511, Department of Industrial Engineering building, Faculty of Engineering, Naresuan University, Phitsanulok, Thailand. A proposed experimental loop of the sand-oil separator system is designed as presented in Fig. 5.

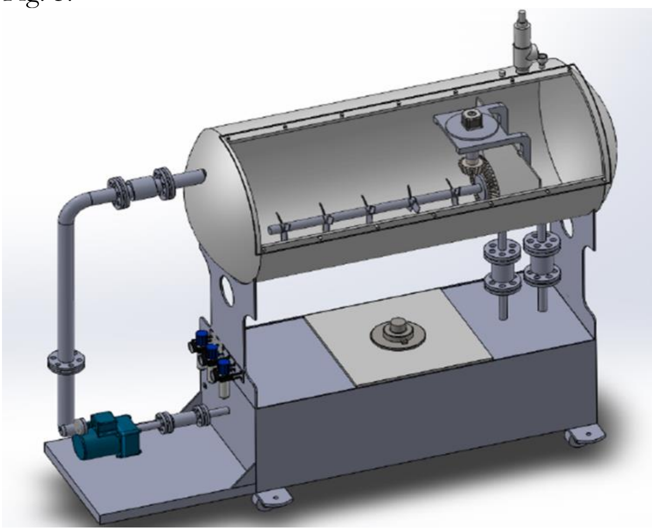

Fig. 5. Experimental loop of lab scaled sand-oil separator system.

The shape of the separator was designed to be a cylindrical vessel corresponding to the pilot plant. The total length of the lab-scale separator was 1200 mm with the inner diameter equal to 600 mm. The separator was constructed from steel and the lid is made from acrylic to permit flow visualization and occupied the area from the centerline on the top of the separator to 300 mm from the bottom of separator (1 quarter). The crude oil reservoir

DOI:10.4186/ej.2022.26.12.1

tanks had a capacity of approximately 400 L. Weir was located between two-hole of water outlet and oil outlet and gap between the weir and each outlet is 20 mm.

A momentum breaker at the inlet was installed to reduce the turbulence caused by the jet of liquid impacting the free surface of the liquid within the vessel. The air compressor was used for controlling the rotational speed of impellers as well as for stirring the impeller inside the crude oil tank. The rotational speed of the impeller was measured by a Laser RPM meter (Tachometer).

The taps were added at both outlet parts to take samples for measuring the efficiency of sand separation. The three-phase fluid of sand-oil-water was circulated from the reservoir tank to the separator using a centrifugal pump, which can support a fluid flow rate of up to 100 L/h. A three-phase mixture of oil-water-sand composition was prepared by volume fraction (55% crude oil, 40% water, and 5% sand).

Fig. 6. Lab scale separator system.

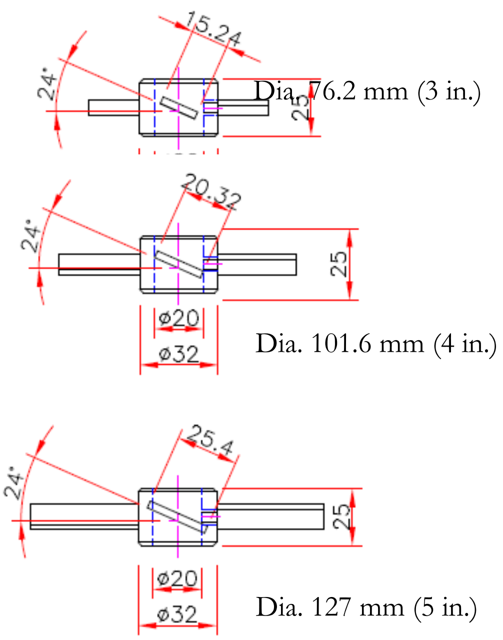

Fig. 7. Sketch of pitched impellers with three blades.

The gas ventilation system was implemented on the right top of the separator using a pneumatic motor. The two separated parts of the crude oil outlet and water outlet will be directly drained to remix in the original crude reservoir with the controlled temperature at 60°C and continuous stirring by 3 blades monitoring by an air compressor.

Design of internal impellers. The shape and sizes of impellers were designed based on [1]. There will be 3 sizes of impellers which are designed as: 76.2 mm (3 in.), 101.6 mm (4 in.), and 127 mm (5 in.) in diameter, and each impeller consist of 3 blades. The pitch angle is fixed to be 24°. The gap between each impeller is adjusted to be 150 mm, 225 mm, and 300 mm for 5 impellers, 4 impellers, and 3 impellers, respectively, as shown in Fig. 7.

For the other blade sizes: the experiment will be done in the same way to compare the separation efficiency.

Crude oil properties. The properties of crude oil, Petroleum oil, sweet crude oil, or Sour crude oil, can be described as follows:

- Flash point: < 120˚F
- Auto-ignition temperature: liquid 450˚F, vapor 800-1000˚F
- Appearance: black liquid
- Specific gravity: 0.80-0.98
- Compositions;

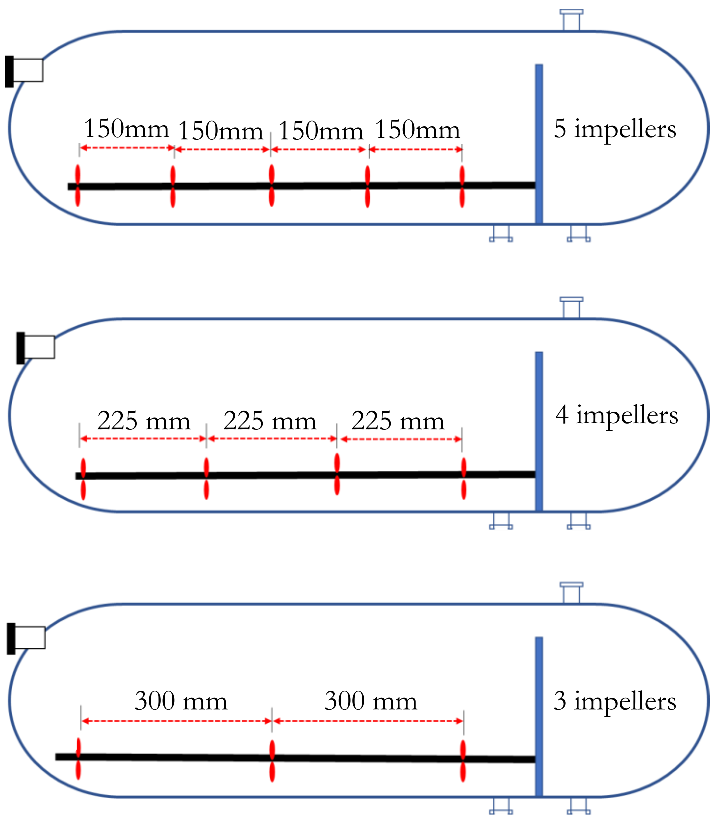

Fig. 8. The 127 mm impeller for different distances and numbers of impellers.

Table 1. Crude oil properties. (Source: Safety Data Sheet: Crude Oil, EP Energy, 06/01/2015) [10].

Components	%wt*
Crude oil (Petroleum)	95-100
Toluene	0-20
Xylenes	0-20
Ethyl benzene	0-4
Benzene	0-2
n-Hexane	0-5
Hydrogen sulfide	Varies

Note: (*) Concentrations are percent by weight, unless the constituent is a gas. Gas concentrations are in percent by volume. Crude oil can contain minor amounts of sulphur, nitrogen, and oxygen-containing organic compounds as well as trace amounts of heavy metals, such as mercury, arsenic, nickel, and vanadium. Naturally occurring radioactive materials (NORM) may also be present. Composition varies depending on the source of the crude oil.

3.2. Experimental Method

Separation testing

1. The storage tank of crude oil was heated at 60°C by the temperature controller.

2. Waiting until the temperature was constant and the crude oil was melted completely.

3. The flow rate of fluid was fixed at the maximum power of the centrifugal pump = 100 L/h.

4. Running the machine and circulating the system for about 30 minutes to stabilize the system before sampling.

5. The rotational speeds of impellers were varied to be 0, 10, 50, 100, and 200 rpm.

Sample Analysis

1. Collect a sample for 3 parts into the glass bottle at different resident times.

- Inlet: 100 ml, 2 bottles (sampling from the drain point of the storage tank)
- Water outlet part: 100 ml, 2 bottles
- Oil outlet part: 100 ml, 2 bottles

2. All samples were filtered using filter paper (Whatman No. 42)

3. Wash the solid part with boiled water.

4. Dry the filtrate in an oven at 100-110°C to evaporate water for 15 minutes.

5. Weigh the dried sand samples.

6. Compare the amount of solid in each part.

4. Computational Fluid Dynamics (CFD)

This process shows the numerical investigation of the 3D hydrodynamics and flows behaviours inside the separator tank using a multiphase CFD method. It consists of four sections in this chapter. First, the fundamental information of software is presented. The modelling approach is basically described for understanding the theory supporting the simulation. The third section informs the numerical procedure of this investigation. Finally, the numerical results obtained from the 3D simulation are presented in the last section.

4.1. Software Information

To obtain effective results, a commercial software name ANSYS was used for this study. ANSYS is one of the effective engineering software that various engineers trust and use as a tool in engineering design procedures. This software can support all disciplines of physics such as flow of fluid, structure mechanics, heat transfer, and electromagnetic. All products namely Fluids, Structures, Electronics, Semiconductors, Embedded Software, Multiphasic are distributed for all engineering problems.

ANSYS is the appropriate program to use as a tool for this research project in part of the numerical simulation that aims to explain the flow phenomena of all substances inside the oil separator modified with a set of impellers. This study ran on the Workbench framework of ANSYS version 19 with Naresuan University's academic research license FLUENT, the most powerful CFD tool in Fluids software of ANSYS products, was chosen for analyzing this CFD application. This program allows us to apply in a wide range of CFD applications and generates acceptance and accurate results including various graphical presentations.

4.2. Modelling Approach

This part of the project aims to investigate the 3D hydrodynamics and flow behavior inside the oil-separator tank including a set of impellers. The flow phenomena inside the tank are combined by the mixed movement of four phases such as air, crude oil, water, and sand. The multifluid VOF model in FLUENT is a hybrid model of the combination between the VOF model and the Eulerian multifluid model. It is suggested to properly use for mixed flow simulation describing the physics of the mixed dispersed phases and the segregated phases.

The volume of fluid (VOF) solver applies one mixed-phase to the conservation of mass and the conservation of momentum. While the hybrid multifluid VOF model separates a set of the mass equation and the momentum equation applying in each phase. It leads to the separation of velocity field solving in each phase. Furthermore, the consideration of the surface tension and the phase interaction through the drag model is integrated into the numerical process. A set of main equations in the Mutifluid VOF model is as follows:

The continuity equation of phase q is expressed as

$$\frac{\partial \alpha_q}{\partial t} + \vec{u}_q \cdot \nabla \alpha_q = 0 \tag{2}$$

The momentum equation of phase q is written as

(3)

$$\frac{\partial(\rho_q\alpha_q\vec{u}_q)}{\partial t}+(\rho_q\alpha_q\vec{u}_q\cdot\nabla)\vec{u}_q = -\alpha_q\nabla p+\nabla\cdot(\mu_q\alpha_q\nabla\vec{u}_q) + \rho_q\alpha_q\vec{g}+\vec{F}_{D,q}+\vec{F}_{s,q}$$

where ρ is density (kg/m3), α is phase fraction, u is phase velocity (m/s), t is time (sec), μ is dynamic viscosity (Pa s), F_D is drag force (N), F_s is surface tension force (N), g is gravitational acceleration (m/s^2)

The volume fraction transport modified with the compression velocity of phase q is defined as

$$\frac{\partial\alpha_q}{\partial t}+\vec{u}_q\cdot\nabla\alpha_q += \nabla\cdot\left(\vec{u}_c\alpha_q(1-\alpha_q)\right)=0 \qquad (4)$$

where $\vec{u}_c = C_\alpha|\vec{u}|\frac{\nabla\alpha}{|\nabla\alpha|}$

$$C_\alpha=\begin{cases}0,no \quad interface \quad sharpening\\ 1,interface \quad sharpening \quad active\end{cases}$$

Moreover, the standard k-ε turbulence model is introduced into the numerical simulation for describing the flow phenomena in turbulence region.

The turbulent kinetic energy equation

$$\frac{\partial(\rho k)}{\partial t}+\frac{\partial}{\partial x}(\rho uk)+\frac{\partial}{\partial y}(\rho vk)+\frac{\partial}{\partial z}(\rho wk) = \frac{\partial}{\partial x}\left[\left(\mu+\frac{\mu_t}{\sigma_k}\right)\frac{\partial k}{\partial x}\right] + \frac{\partial}{\partial y}\left[\left(\mu+\frac{\mu_t}{\sigma_k}\right)\frac{\partial k}{\partial y}\right]+\frac{\partial}{\partial z}\left[\left(\mu+\frac{\mu_t}{\sigma_k}\right)\frac{\partial k}{\partial z}\right]+P_k - \rho(\varepsilon+\varepsilon_c)+\overline{p''d''} \qquad (5)$$

The dissipation rate equation

$$\frac{\partial(\rho\varepsilon)}{\partial t}+\frac{\partial}{\partial x}(\rho u\varepsilon)+\frac{\partial}{\partial y}(\rho v\varepsilon)+\frac{\partial}{\partial z}(\rho w\varepsilon) = \frac{\partial}{\partial x}\left[\left(\mu+\frac{\mu_t}{\sigma_\varepsilon}\right)\frac{\partial \varepsilon}{\partial x}\right] + \frac{\partial}{\partial y}\left[\left(\mu+\frac{\mu_t}{\sigma_\varepsilon}\right)\frac{\partial \varepsilon}{\partial y}\right]+\frac{\partial}{\partial z}\left[\left(\mu+\frac{\mu_t}{\sigma_\varepsilon}\right)\frac{\partial \varepsilon}{\partial z}\right]+c_{\varepsilon1}P_k\frac{\varepsilon}{k} - c_{\varepsilon2}\rho\frac{\varepsilon^2}{k} \qquad (6)$$

where x, y and z are directions of three dimension (m), u, v and w are velocity in x, y and z directions, respectively (m/s), p is pressure (Pa); Prt is turbulent Prandtl number, k is turbulent kinetic energy (m^2/s^2), ε is turbulent dissipation (m^2/s^2)

The production of turbulence P_k is defined as

$$P_k=\mu_t\left\{\begin{aligned}&\left(\frac{4}{3}\frac{\partial u}{\partial x}-\frac{2}{3}\frac{\partial v}{\partial y}-\frac{2}{3}\frac{\partial w}{\partial z}\right)\left(\frac{\partial u}{\partial x}\right)+\left(\frac{4}{3}\frac{\partial v}{\partial y}-\frac{2}{3}\frac{\partial u}{\partial x}-\frac{2}{3}\frac{\partial w}{\partial z}\right)\left(\frac{\partial v}{\partial y}\right)\\&+\left(\frac{4}{3}\frac{\partial w}{\partial z}-\frac{2}{3}\frac{\partial u}{\partial x}-\frac{2}{3}\frac{\partial v}{\partial y}\right)\left(\frac{\partial w}{\partial z}\right)+\left(\frac{\partial u}{\partial y}+\frac{\partial v}{\partial x}\right)\left(\frac{\partial u}{\partial y}\right)+\left(\frac{\partial u}{\partial z}+\frac{\partial w}{\partial x}\right)\left(\frac{\partial u}{\partial z}\right)\\&+\left(\frac{\partial v}{\partial x}+\frac{\partial u}{\partial y}\right)\left(\frac{\partial v}{\partial x}\right)+\left(\frac{\partial v}{\partial z}+\frac{\partial w}{\partial y}\right)\left(\frac{\partial v}{\partial z}\right)+\left(\frac{\partial w}{\partial x}+\frac{\partial u}{\partial z}\right)\left(\frac{\partial w}{\partial x}\right)\\&+\left(\frac{\partial w}{\partial y}+\frac{\partial v}{\partial z}\right)\left(\frac{\partial w}{\partial y}\right)\end{aligned}\right\} \qquad (7)$$

The typical constants in Eq. (5) and (6) are σk = 1.0, σ_ε = 1.3, $c_{\varepsilon1}$ = 1.44 and $c_{\varepsilon2}$ = 1.92. In addition, the turbulent viscosity is expressed as

$$\mu_t=\rho c_\mu\frac{k^2}{\varepsilon} \qquad (8)$$

where c_μ is equal to 0.09.

The semi-empirical correlations to determine the values $\overline{u'}^2$, $\overline{v'}^2$ and $\overline{w'}^2$ are used:

$$\overline{u'}^2=2\alpha_2k \qquad (9)$$

$$\overline{v'}^2=2\alpha_3k \qquad (10)$$

$$\overline{w'}^2=2\alpha_4k \qquad (11)$$

where $\alpha2$, $\alpha3$ and $\alpha4$ are structural scale constants.

The Reynolds stress terms $-\rho\overline{u'v'}$, $-\rho\overline{u'w'}$ and $-\rho\overline{v'w'}$ are given as

$$-\rho\overline{u'v'}=\mu_t\left(\frac{\partial u}{\partial y}+\frac{\partial v}{\partial x}\right) \qquad (12)$$

$$-\rho\overline{u'w'}=\mu_t\left(\frac{\partial u}{\partial z}+\frac{\partial w}{\partial x}\right) \qquad (13)$$

$$-\rho\overline{v'w'}=\mu_t\left(\frac{\partial v}{\partial z}+\frac{\partial w}{\partial y}\right) \qquad (14)$$

The term ε_c and the pressure dilatation term $\overline{p''d''}$ present the compressibility correction are expressed as

$$\varepsilon_c=\gamma_1M_t^2\varepsilon \qquad (15)$$

$$\overline{p''d''}=-\gamma_2P_kM_t^2+\gamma_3\rho\varepsilon M_t^2 \qquad (16)$$

where $M_t=\sqrt{2k/a_s^2}$ is the turbulent Mach number, a_s as is the speed of the sound (m/s), the constant values are γ_1 =1.0, γ_2 = 0.4 and γ_3 = 0.2.

4.3. Numerical Simulation Procedure

For 3D simulation, the simplified 3D geometric model created via the Design Modeler in ANSYS was detailed in the dimensions of the laboratory scale of an oil separator attached with a system of five impellers. Then an effective mesh of about 3,404,816 cells leading to the accepted results with the minimum computing time was constructed throughout Meshing in ANSYS.

The simulation was performed in FLUENT with the Multifluid VOF model and the k-ε turbulence model. Air was defined as the primary phase while Crude oil, Water, and Sand with a particle diameter of 45 microns were the secondary phases. The rotation motions due to all impellers introduced the rotation reference frame (RMF) method integrated into the simulation setting. All parameters and boundaries conditions required for solving were completely

DOI:10.4186/ej.2022.26.12.1

informed with the condition of the experimental setup shown in 3. Research Methodology. The volume fraction of mixed-phase (55 % crude oil, 40 % water, and 5 % sand) flows at 0.25 litter/s. was defined as the inlet velocity of the system. The oil separator ran at the normal atmospheric pressure. The initial condition of sand sedimentation at a thickness of 0.02 m, the water layer height of 0.16 m, and the crude oil layer height of 0.22 m from the bottom surface of the tank. The constant impeller speeds of 0, 10, 50, 100, 200, 300 rpm were put in the operating conditions of the simulation. The computational simulation was defined in the steady-state condition. Each calculation process in a time step was continuously performed until reaching the convergence or the maximum of 5,000 iterations. However, the criteria convergence was defined at 0.0001. Additionally, several parameters such as the volume fraction of each phase, the mass flow rate of the phase input and output, and the pressure were monitored and collected for the post-processing step.

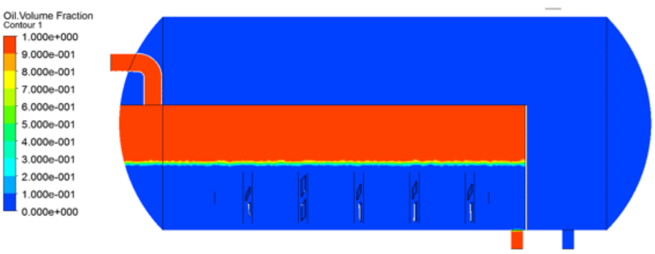

(a) Oil volume fraction

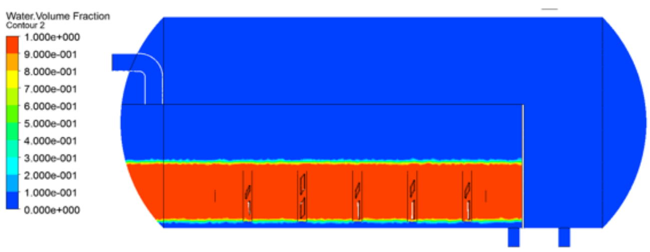

(b) Water volume fraction

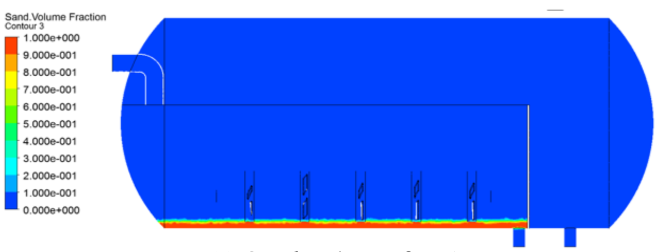

(c) Sand volume fraction

Fig. 9. Contour of the phases in the vertical cross-section located at the Z coordinate at the initial process without rotation of impellers (0 rpm)

4.4. Numerical Simulation Results

Actual hydrodynamic flow from CFD simulation. This section presents the numerical results obtained from the CFD analysis of the fluid flow in the modified oil separator installed with a set of impellers. Modelling results of moving phenomena of all fluid phases inside the separator via ANSYS software at several times are analysed and presented in Fig. 9, Fig. 10.

In Fig. 9, the beginning step of feeding the fluid into the separator without rotation of the impeller is displayed. Fig. 9 (a) shows the red band located at the top layer represents the crude oil phase and is separated from the water part by flowing across the weir to collect in the storage tank. In Fig.9 (b), the red band shows the water layer located between the water layer and sand layer. The sand layer is located at the bottom of the separator as shown by the red band in Fig.9 (c). The rotation speed of the impeller is 0 rpm yielding the sand packing smoothly in the bottom of the separator.

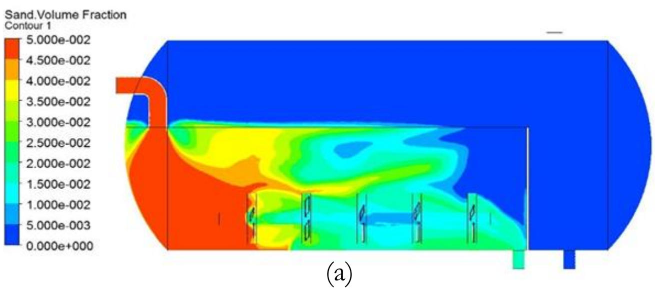

(a)

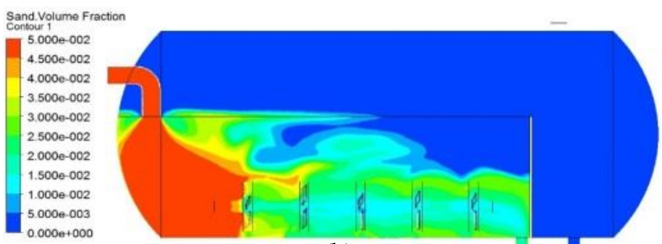

(b)

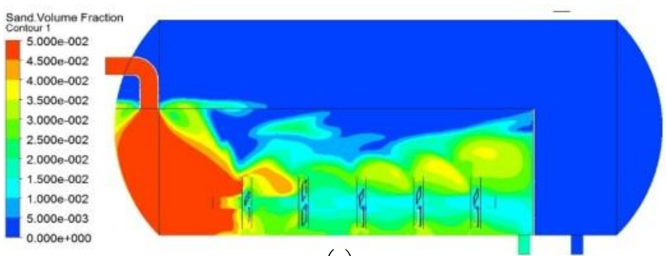

(c)

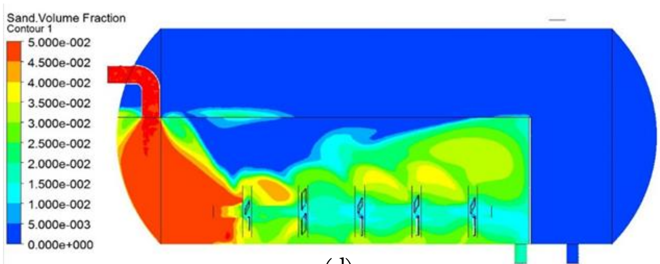

(d)

Fig. 10. Contour of the phases in the vertical cross-section located at the Z coordinate at different rotation speeds: a) 50 rpm, b) 100 rpm, c) 200 rpm, and d) 300 rpm.

Fig. 10 (a-d), it was found that the rotation speed of impellers (50 rpm – 300 rpm) affected the turbulent flow of sand particles. The sand particles disperse strongly to the water layer and oil layer when increasing the rotation speed of the impeller but it is still located on the left side of the separator which did not cross the weir and did not make the contamination of the produced oil. This can be pointed out that the separator coupled with internal impellers leads to prevent sand sedimentation in the separator effectively. These numerical results represent the transport phenomena in detail where it could support the flow pattern obtained from the laboratory-scale experiment.

Effect of rotation speed of impellers. The amount of sand outlet in the water phase with various rotation speeds resulting from CFD simulation is shown in Table 2. The rotation speeds of impellers were varied as 0, 50, 100, 200, and 300 rpm. It was found that amount of sand removal by 50 rpm speed of impellers is higher than that of 0 rpm (as without impeller). When the rotation speed is increased to 100, 200, and 300 rpm, the amounts of the sand outlet were also constantly increased, e.g. at 300 rpm, it gives the highest amount of sand outlet followed by 200, 100, 10, 50, and 0 rpm, respectively. When considering in terms of %Efficiency of sand removal with impeller rotation speed compared to 0 rpm, it was found that 50 rpm speed gave dramatically higher efficiency of sand removal than 0 rpm for 179%. When the rotation speeds were increased slightly to 100, 200, and 300 rpm, the efficiencies also dramatically grew to 191%, 205%, and 219%, respectively.

Table 2. Results of sand outlet in water part from different rotation speeds and efficiency of sand removal in different rotation speeds compared with 0 rpm.

Rotation speed (rpm)	Sand outlet in water (g)	% Efficiency of sand removal
0	0.76	-
50	2.12	179%
100	2.22	191%
200	2.32	205%
300	2.43	219%

In Fig. 11, if we evaluate the %efficiency of sand removal from 0 rpm to 50 rpm, it could be seen that the % efficiency is shapely increased as accelerating speed to 50 rpm. When the speeds were increased to 100, 200, and 300 rpm, the % efficiency is slightly higher than that from 50 rpm but not so much significantly different. For example, at 300 rpm, % efficiency is about 219% which is higher than that of 200 rpm only 14%, when compared to the % efficiency of 50 rpm which is higher than that at 0 rpm for 179%. This issue could make us decide the proper impeller speed. If we need to save energy, we would use the speed in the range of 50-200 rpm which could be enough to eliminate sand from the produced oil effectively.

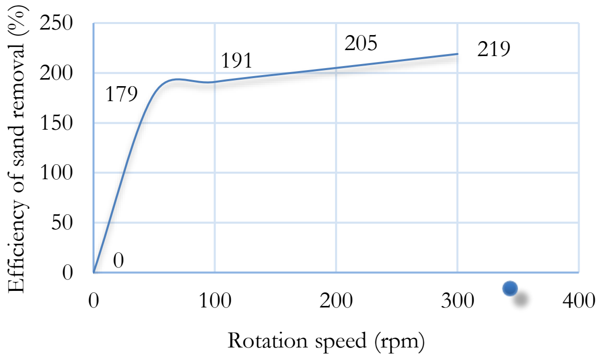

Fig. 11. Percent efficiency of sand removal in different rotation speeds compared with 0 rpm.

5. Results and discussion

Results and discussion in a part are the effect of impeller size on the sand removal, effect of the impeller on oil-water phase separation, effect of the rotation speed of impeller on the sand removal, effect of duration time on the pattern of sand movement as follows:

Table 3. DOE of different rotation speed and sampling time for 3 inch-diameter of impellers.

Sampling time (min)	Rotation speed	Sample No.	Partied (Crude Inlet) (g)				Particle (Water outlet) (g)			
			Filter	Filter + sand	Sand	Average	Filter	Filter + sand	Sand	Average
30	10	1	44.6138	44.7929	0.1791	0.1465	43.8861	44.4456	0.5595	0.3334
		2	46.3490	46.4628	0.1138	0.1465	45.4752	45.5825	0.1073	0.3334
	50	1	44.6758	50.1433	5.4675	2.7338	46.2913	46.6002	0.3089	0.1545
	100	1	44.6707	45.2477	0.5770	0.7356	45.2906	45.4187	0.1281	0.1842
		2	46.2883	47.1825	0.8942	0.7356	45.4717	45.7120	0.2403	0.1842
	200	1	44.0681	44.0958	0.0277	0.0138	43.8698	44.0413	0.1715	0.1442
		2	44.0681	44.0958	0.0277	0.0138	46.2206	46.3375	0.1169	0.1442
60	10	1	46.3263	46.3727	0.0464	0.0232	43.5938	44.6471	1.0533	0.5267
	50	1	45.2931	45.3076	0.0145	0.0270	44.6757	45.9168	1.2411	0.6206
		2	46.2886	46.3281	0.0395	0.0270	44.6757	45.9168	1.2411	0.6206
	100	1	43.6080	43.6323	0.0255	0.0340	43.8698	44.1055	0.2357	0.1580
		2	46.3230	46.3654	0.0424	0.0340	44.6058	44.6861	0.0803	0.1580
	200	1	46.2334	46.6683	0.4349	0.2174	45.4598	45.5072	0.0474	0.0237

Table 4. DOE of different rotation speed and sampling time for 5 inch-diameter of impellers.

Sampling time (min)	Rotation speed	Sample No.	Partied (Crude Inlet) (g)				Particle (Water outlet) (g)			
			Filter	Filter + sand	Sand	Average	Filter	Filter + sand	Sand	Average
30	0	1	44.7033	44.7994	0.0961	0.0837	46.2584	46.4038	0.1454	0.0903
		2	43.6359	43.7072	0.0713	0.0837	44.6403	44.6755	0.0352	0.0903
	10	1	43.9097	45.0884	1.1787	0.8550	45.4055	47.3968	1.9913	1.7173
		2	44.5124	46.0438	0.5314	0.8550	44.7221	46.1654	1.4433	1.7173
	50	1	44.2855	52.8387	8.5532	4.2766	44.7041	45.1789	0.4748	1.0423
		2	0	0	0	4.2766	43.6540	45.2639	1.6099	1.0423
	100	1	43.9236	69.4229	25.4993	19.3390	44.1149	44.5536	0.4387	0.7038
		2	45.3446	58.5233	13.1787	19.3390	45.2073	46.1762	0.9689	0.7038
	200	1	43.6498	56.3397	12.6899	16.2152	45.3411	46.5817	1.2406	0.9389
		2	44.1084	63.8453	19.7405	16.2152	45.2033	45.8404	0.6371	0.9389
60	0	1	45.2093	49.3424	4.1331	2.4568	43.9417	48.6710	4.7293	4.0007
		2	44.1395	44.9200	0.7805	2.4568	45.4545	48.7265	3.2720	4.0007
	10	1	45.4230	51.6664	6.2434	3.3772	45.2694	47.5076	2.2382	1.8913
		2	43.5931	44.1040	0.5109	3.3772	46.2202	47.7645	1.5443	1.8913
	50	1	44.0480	44.1105	0.0625	0.1850	43.8510	44.8231	0.9721	2.4967
		2	45.3771	45.6845	0.3074	0.1850	45.1469	49.1682	4.0213	2.4967
	100	1	45.4638	45.5714	0.1076	0.0795	45.3001	46.9521	1.6520	1.8247
		2	43.6207	43.6721	0.0514	0.0795	46.2430	48.2403	1.9973	1.8247
	200	1	45.3352	45.3488	0.0136	0.0125	44.3033	45.2114	0.9081	2.0111
		2	46.2887	46.3001	0.0114	0.0125	43.6901	46.8042	3.1141	2.0111

5.1. Effect of Impeller Size on the Sand Removal

In the part of the experiment, the diameter of impellers was studied to examine the most appropriate size of the impeller by comparing between 3 and 5 inch-diameter in various rotation speeds (10, 50, 100, and 200 rpm) of impellers and different sampling times (30 and 60 min). The design of the experiments (DOE) was shown in Tables 3. - 4.

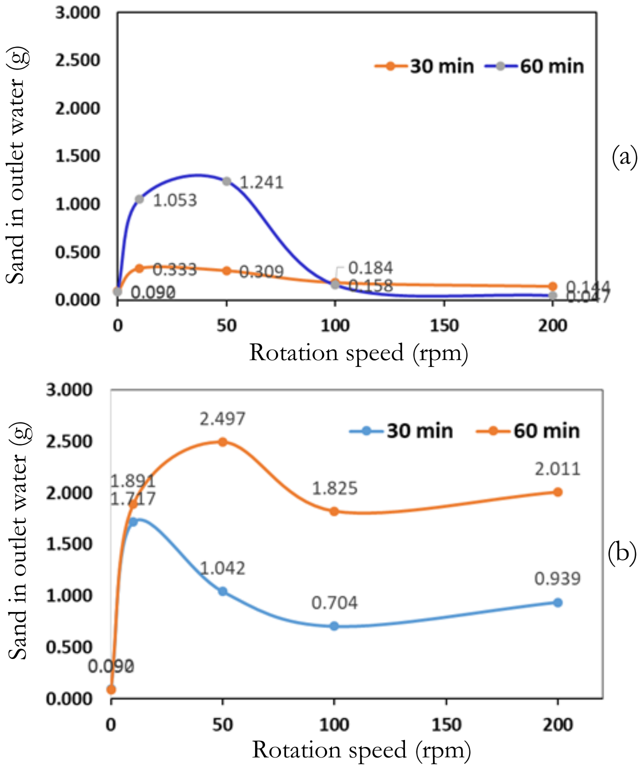

Fig. 12. Comparison of rotation speed for different impeller size in diameter: (a) 3 inch-impeller and (b) 5 inch-impeller.

From the results shown in DOE Table 3. – 4., it could be extracted into Fig. 12. and 13. to make it clearer comparison of impeller size between 3 and 5 inch diameter. It was found that the condition of “5 inch impeller, 50 rpm, and 60 min” yielded the highest efficiency for sand separation from outlet water. The 5 inch impeller yields the outlet sand better than the 3 inch-impeller, the running time for 60 minutes yields the outlet sand higher than 30 minutes, the speed 50 rpm yields the most sand outlet without any sand coming out in the crude oil part. From this result, it could be concluded that the bigger the impeller size, the more effective sand removal as it generate more turbulence for sand movement to the outlet channel. Therefore, 5 inch impeller was taken as the best optimum size to use for the further experiment without any needed test of 4-inch diameter.

5.2. Effect of Impeller on Oil-water Phase Separation

From the results in DOE Table 3. and 4., it can be clearly seen that there is no water and sand particle contaminated in the crude-oil outlet. Therefore, it could believe that the crude oil obtained at the separator outlet is purified. The separator modified with impellers did not interfere phase separation of oil and water. In addition, the rotation of impellers still maintains sand particles staying along with water level without any

DOI:10.4186/ej.2022.26.12.1

flowing up to the oil level as can be seen clearer in Fig. 10. It can be observed that the movement activity of sand particles occurred only in the water phase and it was quite difficult to reach to oil level since the level of water in the crude (volume fraction of water is 40%) is high enough to cover the area of sand movement.

5.3. Effect of rotation speed of impeller on the sand removal

To determine the optimum rotation speed of the impeller, the experiments were performed with varying the rotation speed as 0, 10, 50, 100, 200 rpm to plot against the sand outlet in various sampling times for 5 intervals at 0, 15, 30, 45, 60 min, using the impeller diameter with 5 inches. The DOE was resulting and the experimental results were shown as a plot in Fig. 14.

From the plot in Fig. 14., rotation speeds of 10 and 50 rpm show similar trends without any sand out whether how long the time pass, while 0 rpm shows a little outlet at 30 min. Considering rotation speed at 100 rpm, the level of the sand outlet has somewhat fluctuated, e.g. it gradually grows up until 30 min, then slightly falls down at 45 min and rises again at 60 min.

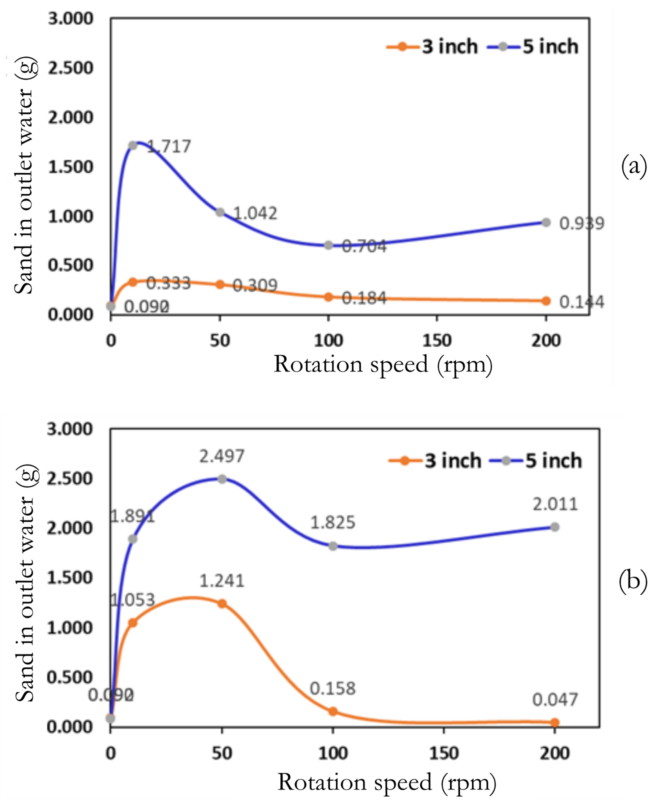

Fig. 13. Comparison of rotation speed for different sampling time: (a) 30 min and (b) 60 min.

Considering at 200 rpm, the amount of sand outlet increases sharply from zero to about 3 g in 15 min and suddenly falls down throughout 60 min. Overall, it could be seen that, when the speed of rotation is increased, the sand outlet also increases. This might result from the packing of some part of sand dune at the bottom of the separator. Probably, the packed sand dune needs as high the speed of rotation to drive its move to the outlet channel as shown in the experimental results. These results have definitely corresponded to the CFD results shown in Table 2. This relates to the fact that a high speed of rotation will create turbulence flow of fluid causing sand dune at the bottom of the separator. The maximum speed of impeller rotation in our system is 200 rpm due to the limitation of pressure controller efficiency.

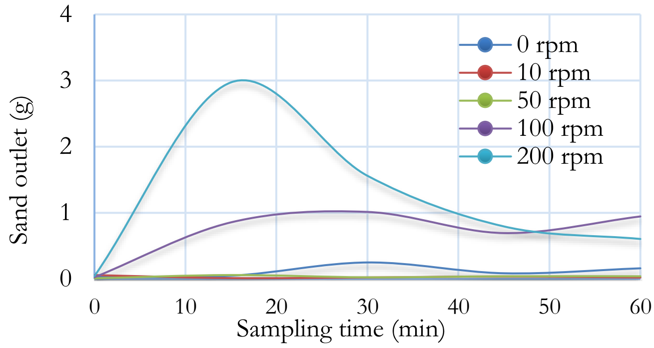

Fig. 14. Sand outlet from different rotation speeds against sampling times.

In order to confirm these results, we operated repeating experiments with the same conditions by continuing the system from the previous run as displayed in DOE of different rotational speeds in various sampling times. The result's plot is shown in Fig. 15.

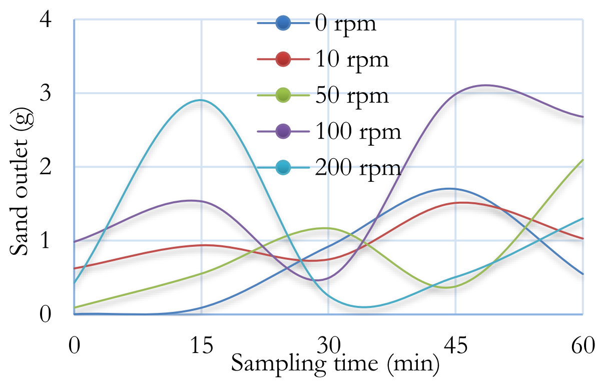

Fig. 15. Sand outlet from different rotation speeds in various Sampling times.

Regarding sampling time at 0 min, some curves did not start at zero level of sand outlet, this is because there is some sand remained in the bottom of the system. Considering the whole plot, the trends of all curves are changed and obviously fluctuate like wavy patterns. However, when comparing the rotation speed of the impeller, it still remains the same trend as the previous experiments. The sand outlet rises with increasing the speed of impeller rotation, e.g. at 200 rpm, it gives the highest amount of sand out following by 100, 10, 50, and 0 rpm, respectively.

These phenomena could be explained from the theory of sand deposition in the horizontal system [8] corresponding to the laminar and turbulent flow. The report proposed a simple equation used to evaluate the molecular diffusivity of the mixture as follows equation (1), the diffusivity (D) of sand depends on the size (d) of sand and the average velocity (u') of the mixture between sand and fluid. If the size of sand increases and the average velocity increase, the diffusivity will be increased. This equation could be applied to our results that when the sand and the fluid velocity increase in terms of the increasing rotation speed of the impeller with a constant average particle size of about 45 microns. Fig. 15. This shows that the sand diffusivity also increases as shown in terms of sand outlet in a wavy curve pattern lasting 60 minutes, which was also in agreement with the CFD speed results presented in Table 2.

For this stage, it could be imagined for the real situation that, when we flow crude oil for a very long time without clearing the old system, the sedimentation of sand occur continuously, this makes an increasing amount of sand and higher-level packing in the bottom of the separator and the amount of sand in the storage tank was also lower comparing to the beginning stage. Before doing the next experiment, we tried to eliminate all the residual sand in the system. At this moment, it was found that there was very little amount of sand remaining at the bottom of the separator. It would be confident that the system is effective to prevent sand packing. Furthermore, this makes sure that our system now is now set as original and ready for the next running.

5.4. Effect of duration time on the pattern of sand movement

In this part, the longest-running of experiments was performed to confirm the real pattern of the curve by extending the time of operation to 300 min and sampling every 15 min. The DOE of Sand outlet for 300 min and the plot to data in Fig. 16. respectively.

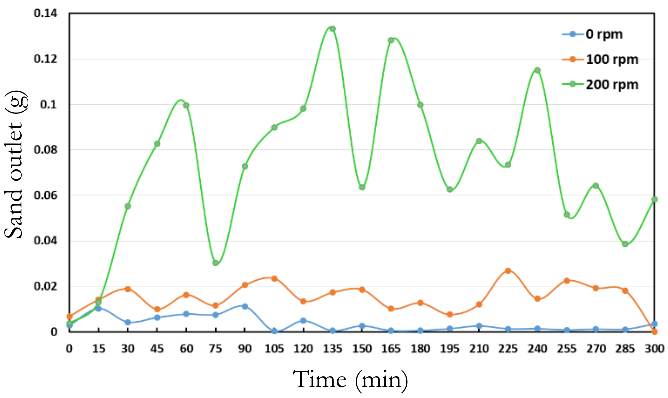

Fig. 16. The experimental data of sand outlet in each time of operation.

In Fig. 16, the curve obviously shows a wavy pattern constantly. At the first 60 min, at 200 rpm speed, sand out drastically rises to maximum peak at 60 min and suddenly drops at 75 min. This also shows the same shape both in the case of 0 and 100 rpm. The amount of sand outlet from 200 rpm is significantly higher than that of 0 and 100 rpm speed. This can additionally approve that 200 rpm is the optimal rotation speed of the impeller. Considering the whole curve of 200 rpm for 300 min running, it can be seen that the curve is stably moving like a wave characteristic which was predicted based on the previous results. These results have also corresponded to CFD simulation as displayed in Fig. 10. The pattern of sand dunes was created by the rotation of impellers. When the amount of sand was accumulated into the optimum level in addition to the driving force from the impellers, the sand will move to the outlet channel as it shows in the shape of an up and down curve.

In addition, the profile of this curve can be explained by experiments and theory which is corresponding to a previous publication [5]. Three-phase flow (air, water, sand) in a horizontal pipeline was studied. It was found that the gas ratio did not affect the average dune front velocity. The saltation mechanism and the pattern of sand dune formation can be described in Fig. 13. The saltation mode can be characterized which strongly influenced by the dynamic of sand transportation and blockage process. They also mentioned that at the critical velocity U_c, the sand particle is entrained from the stationary layer, transported along the pipe, and generated the bed-load as displayed in Fig. 17(a). Above the critical velocity, particles are occasionally raised up the bed interface. But the fluid force is not strong enough to maintain the grains in suspension; therefore, the sand particles fall and hit the other grains that repeated the process of sand dune formation which is illustrated in Fig. 17(b). The saltation occurred due to gravitational forces.

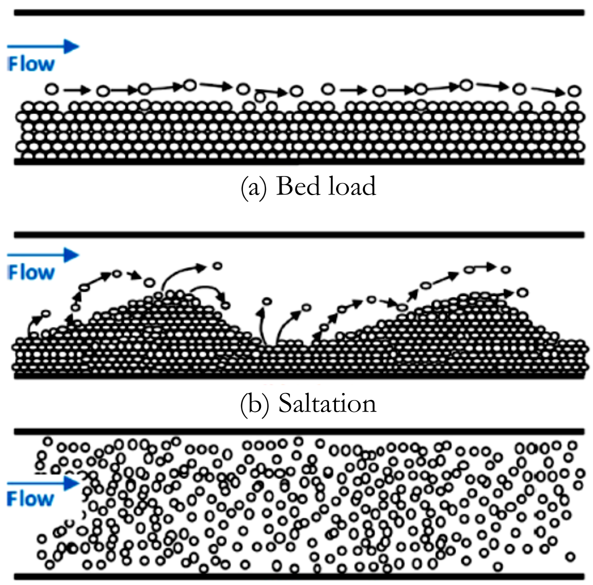

(a) Bed load

(b) Saltation

(c) Suspension

Fig. 17. Sand formation inside liquid/solid pipeline [5].

The velocity of intermittent flow depends on gravitational acceleration. Danielson [11] used the SINTEF database to obtain the following relation for the critical velocity. The critical velocity wrote as;

$$U_c = Kv^{-n/(2-n)} d^{n/(2-n)} (gD(s-1))^{1/(2-n)} \quad (17)$$

where d = the sand particle diameter, D = the pipe diameter, g is the acceleration due to gravity, S = the ratio of sand particle to carrier fluid density, K and n are equal to 0.23 and 1/5.

It was found that the flow rate influences the structure of sand dunes. For higher flow rates the length of the sand dune decreases in the system the frequency of dune increases. The pattern of sand dunes monitored by CCD recording showed in Fig. 18.

Finally, it is clearly said that the numerical results obtained from the computational simulation could fairly explain the flow phenomena of all phases especially the sand movement created from the experiment. It is possible to use the CFD as a tool with the consideration of computing time for optimal design procedure.

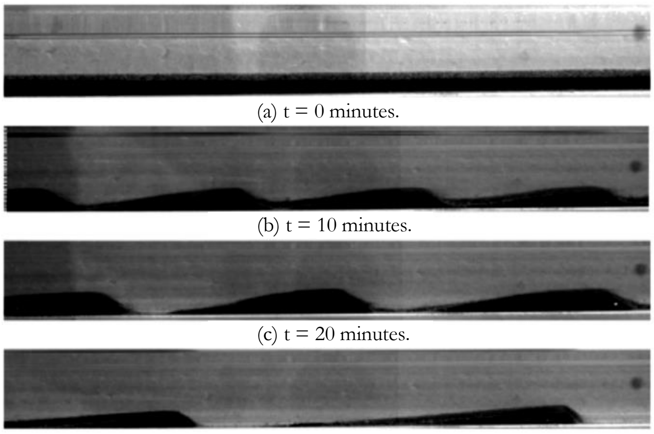

Fig. 18. The pattern of dunes in each time steps.

6. Conclusions

The new design of an advanced separator with additional impellers was successfully implemented in the laboratory prototype. The efficiencies of additional impellers to prevent sand deposition were investigated through CFD simulation and laboratory experiments.

For the CFD model, it was performed via the steady-state for 300 min. The flow phenomena of the fluids were presented that the accumulation of sand packing bed near the outlet channel including rotation of impellers affects the efficiency of sand removal from the separator. The %Efficiency of sand removal increased with increasing the speed of impellers as 50-300 rpm. The efficiency of oil-water phase separation was not disturbed by the rotation of the impeller. This indicates that the separator system with internal impellers leads to effectively prevents sand sedimentation in the advanced separator.

In the laboratory experiments, the results show that 5 inch-impeller is the optimum size for preventing the sand packing in this system. The rotation speed of 200 rpm generated the most performance for sand removal compared to 0, 50, and 100 rpm. Duration time of operation in the lab experiment was 300 min to observe the real profile of the sand outlet. The stable wavy characteristic of the sand outlet curve was obtained in all cases of rotation speeds. We found the limitation of our prototype system is that the flow rate of sand into the separator was not stable and could not be absolutely controlled.

Recommendations for further research in the future are;

1) Install IoT instrument as well as Computer Control System which include measurement of sand by visualization technology and printout in the computer for measurement of separation efficiency.

2) Find out and optimization of system performance efficiency in the new design of advanced separator by using the computerized application.

3) Develop and implement the new design of advanced separator in offshore/onshore (field area) application and our design optimization.

Acknowledgement

This research was supported/partially supported by the Exploration and Production Public Company Limited (PTTEP), Thailand. We thank our colleagues from PTTEP and Naresuan University, Faculty of Science and Engineering who provided insight and expertise that greatly assisted the research, although may not agree with all of the interpretation/ conclusions of this paper.

We thank Dr. Thana Slanvetpan, Senior Engineer of PTTEP for assistance with the Separator technique, methodology and Mr. Surachai Lamsunthia, PTTEP for comments that greatly improved the research.

Finally, thanks to the Faculty of Engineering at Naresuan University. They gave scholarships to support the study of graduate students (Ph.D.) to Mr. Somchai Kongnoo, who was responsible for some of the research and articles in this paper.

References

[1] I. Fořt, T. Jirout, R. Sperling, S. Jambere, and F. Rieger "Study of pumping capacity of pitched blade impellers," *Acta Polytechnica*, vol. 42, no. 4, pp. 68-72, 2002.

[2] M. J. H. Simmons, E. Komonibo, B. J. Azzopardi, and D. R. Dick, "Residence time distributions and flow behavior within primary crude oil–water separators treating well-head fluids," *Chemical Engineering Research and Design*, vol. 82, no. 10, pp. 1383-1390, Oct. 2004.

DOI:10.4186/ej.2022.26.12.1

[3] I. Bibobra and S.Okotie, "Effect of sand invasion on oil well production: A case study of garon field in the Niger Delta," *The International Journal of Engineering and Science (IJES)*, vol. 4, no. 5, pp. 64-72, 2015.
[4] J. Guo, D.-T. Gong, J. Zhang, L.-Y. Wang, Z.-C. Zheng, and K.-M. Li, "Studies on mechanism of sand removal from crude oil," *Journal of Hydrodynamics Ser. B*, vol. 18, no. 3, pp. 394-399, Jul. 2006.
[5] A. Goharzadeh, P. Rodgers, and C. Touati, "Influence of gas-liquid two-phase intermittent flow on hydraulic sand dune migration in horizontal pipelines," *Journal of Fluids Engineering*, vol. 132, no. 7, Jul. 2010.
[6] F. Farias, J. S. Ouza, W. Lima, A. Macêdo, S. Neto, and A. Lima, "Influence of geometric parameters of the hydro cyclone and sand concentration on the water/sand/heavy-oil separation process: Modeling and Simulation," *The International Journal of Multiphysics*, vol. 5, no. 3, pp. 187-202, Sep. 2011.
[7] S. A. I. Bellary and A. Samad, "Pumping crude oil by centrifugal impeller having different blade angles and surface roughness," *Journal of Petroleum Exploration and Production Technology*, vol. 6, no. 1, pp. 117-127, 2016.
[8] S. Sanni, O. Surajudeen Adegboyega, S. S. Adefila, and M. Emetere, "Theoretical study of sand entrainment and deposits in horizontal oil transport," *Science Research*, vol. 3, no. 6, pp. 314-323, 2015.
[9] H. Zhang, Y. Liang, X. Yan, B. Wang, and N. Wang, "Simulation on water and sand separation from crude oil in settling tanks based on the particle model," *Journal of Petroleum Science and Engineering*, vol. 156, pp. 366-372, Jul. 2017.
[10] *Safety Data Sheet: Crude Oil*, EP Energy, June 1st, 2015, pp. 1-9.
[11] T. J. Danielson, "Sand transport modeling in multiphase pipeline," in *Offshore Technology Conference*, Houston, Texas, 2007.

Kawin Sonthipermpoon was born in Phitsanulok city,Thailand in 1964. He received B.S.degree in Physics from Srinakarinwirot Phisanulok campus, Thailand in 1985 and M.Eng. degree in Electrical Engineering from King Mongkut's Institute of Technology Ladkrabang (KMITL), D.Eng. in Manufacturing Systems Engineering from Asian Institue of Technology (AIT), Thailand and more in post-doctoral in Manufacturing Engineering from Hannover University, Germany.

From 2005 - onwards, Associate Professor, Naresuan University, continue duties: Research in the field of Computational Fluid Dynamics (CFDs), Renewable energy such as Dish-Stirling Energy Systems. CNC machining application and CAD/CAM/CAE design, Enterprise Resource Planning (ERP), Information Technology as well as Robotics application and Smart Manufacturing Systems Engineering.

Kwanchai Kaitong, currently Associate Professor at Department of Mechanical Engineering, Faculty of Engineering Naresuan University, Muang, Phitsanulok, Thailand. He received B.Eng. in Mechanical Engineering from Chaingmai University in 1994, M.Eng. in Mechanical Engineering from Chaingmai University in 1999, Ph.D. in Mechanical Engineering, University of Northumbria at Newcastle, UK in 2012.
Research in the field of Thermal Engineering, Numerical Modeling, Computational Fluid Dynamics (CFDs), Design of Stirling Engine.

Wikorn Punyain, currently Associate Professor at Department of Chemistry, Faculty of Science and Research Center for Academic Excellence in Petroleum, Petrochemical and Advanced Materials, Naresuan University, Muang, Phitsanulok, Thailand. He received B.Sc. in Chemistry from Chiangmai University in 2001, M.Sc. in Physical Chemistry from Mahidol University in 2006, Dr.rer.nat. in Chemistry from Graz University of Technology, Austria in 2011.

Research in the field of Computational Studies of the Novel Sunscreen Compounds, Computational Studies of Atmospheric Chemistry, Theoretical Investigations of Weak Interaction in Water Cluster – Halogen Anion Complexes.

Yupin Phuphuak, currently Associate Professor at Department of Chemistry, Faculty of Science, Naresuan University, Muang, Phitsanulok, Thailand. She received B.Sc. in Chemistry from Ubon Ratchathani University in 2005, M.Eng. in Chemical Engineering from Thammasat University in 2009, Ph.D. in Petrochemical Technology, Petroleum and Petrochemical College from Chulalongkorn University in 2013.

Research in the field of Polymer Synthesis and Funtionalization, Polymerization Catalyst and Mechanism, Biodegradable Polymers.

Somchai Kongnoo was born in Phichit, Thailand in 1978. He received the B.I.Ed. Industrial Engineering from Pathumwan Institute of Technology in 2003, M.Eng. Management Engineering from Naresuan University in 2013. The present studying a Ph.D. in Management Engineering at Naresuan University, Thailand.

From 2000 to 2011, he was a Design Engineer in Pichit Industrial Works Co., Ltd. Present is Schunk Carbon Technology Co., Ltd. (Schunk Group). The company is an industry about product manufacturing, automobile parts. Responsibilities about mechanical machine design, tooling design, CAD/CAM/CNC, manufacturing process. The last position is Engineering Design Manager. Since 2011, he has been a teacher at Phitsanulok Technical College in the Production Machine Tool Department.